

## Central peak and narrow component in x-ray scattering measurements near the displacive phase transition in SrTiO<sub>3</sub>

Hawoong Hong,<sup>1</sup> Ruqing Xu,<sup>2,3</sup> Ahmet Alatas,<sup>1</sup> M. Holt,<sup>1</sup> and T.-C. Chiang<sup>2,3</sup>

<sup>1</sup>Advanced Photon Source, Argonne National Laboratory, 9700 South Cass Avenue, Argonne, Illinois 60439, USA

<sup>2</sup>Department of Physics, University of Illinois, 1110 West Green Street, Urbana, Illinois 61801-3080, USA

<sup>3</sup>Frederick Seitz Materials Research Laboratory, University of Illinois, 104 South Goodwin Avenue, Urbana, Illinois 61801-2902, USA

(Received 3 September 2008; revised manuscript received 10 September 2008; published 30 September 2008)

The second-order displacive phase transition in SrTiO<sub>3</sub> at  $T_C \sim 105$  K has been the subject of much debate. For temperature  $T$  above and near  $T_C$ , energy scans by neutron scattering have shown a central peak (CP) at the  $R$  point in the Brillouin zone in addition to a pair of soft phonon peaks, while momentum scans by x-ray thermal diffuse scattering around the  $R$  point have shown a narrow component (NC) atop a broad thermal peak caused by the soft mode. This work clarifies the relationship between the CP and NC by inelastic x-ray scattering with high energy and momentum resolutions. The CP and NC are derived from the same origin and can be attributed to defect-induced local transition above  $T_C$ .

DOI: [10.1103/PhysRevB.78.104121](https://doi.org/10.1103/PhysRevB.78.104121)

PACS number(s): 64.70.kp, 61.05.cf

### I. INTRODUCTION

The prototypical perovskite SrTiO<sub>3</sub> exhibits a displacive phase transition at  $T_C \sim 105$  K with unusual features.<sup>1–3</sup> Its behavior has attracted much interest for possible generic implications regarding the properties of complex oxides in general. As  $T$  approaches  $T_C$  from above, the lowest transverse-acoustic phonon mode at the  $R$  point in the Brillouin zone softens and turns into a frozen lattice distortion at  $T \leq T_C$ , which involves antirootations of neighboring oxygen cages. Neutron scattering (NS) was able to follow the soft mode for the most part, but the energy scans became dominated by a central peak (CP) before the transition set in at  $T_C$ .<sup>4–6</sup> X-ray thermal diffuse scattering (TDS), on the other hand, revealed a narrow component (NC) at the  $R$  point in reciprocal space sitting atop a broad thermal peak caused by the soft mode.<sup>7,8</sup> The CP and the NC are not accounted for by the standard phase transition theory including renormalization effects, and their physical origins have been under intense debate.<sup>9–13</sup> While it is natural to speculate a certain connection between the two, a very careful study by NS failed to detect a NC,<sup>6</sup> even though it should have been a prominent contribution based on corresponding x-ray TDS measurements.<sup>12</sup> The same NS study also showed a significant width of the CP in reciprocal space, thus implying that the broad component in TDS might contain a significant elastic contribution. A recent high-resolution x-ray speckle measurement provided evidence that the NC and CP were both static features but suggested that the two were likely related to different types of imperfections involving different length scales.<sup>13</sup>

Thus far, the experimental results do not come together to provide a coherent, seamless picture. To clarify this outstanding issue, we have performed high-resolution inelastic x-ray scattering (IXS) measurements. This method provides information similar to NS but can be carried out with a much better resolution in reciprocal space. Furthermore, its probing depth is directly comparable to that of x-ray TDS; thus, the NC and CP observed by the two x-ray methods can be compared on the same footing. By contrast, NS probes a large sample volume of  $\sim 1$  cm<sup>3</sup>, which is about five to six orders

of magnitude larger than that probed by x-rays. Like NS findings, our IXS results show a CP that becomes very intense near  $T_C$ . However, in sharp contrast to NS findings, we find the CP component to have a very narrow width centered about the  $R$  point in reciprocal space, with a rapidly decaying and negligibly small tail within the main body of the TDS broad component. These results, as well as other evidence, conclusively establish that the CP and NC as observed by x-ray scattering are derived from the same elastic-scattering mechanism and that the broad component is essentially all inelastic. The differences compared to NS results will be discussed.

### II. EXPERIMENTAL DETAILS

Our IXS measurements were performed at the undulator beamline of Sector 3 at the Advanced Photon Source, Argonne National Laboratory.<sup>14,15</sup> A single crystal of SrTiO<sub>3</sub> purchased from MTI Corp. was used as the sample. The crystal had a dimension of  $1 \times 1 \times 0.05$  cm<sup>3</sup> and was optically clear and colorless with a well-polished surface. Such crystals are typically employed as substrate materials for oxide epitaxial layer growth. The incident x-ray energy was set at 21.657 keV. The overall energy resolution was 2.09 meV (full width at half maximum) as determined by elastic scattering from a piece of amorphous plexiglass and by the measured width of a Bragg peak of SrTiO<sub>3</sub>. The sample temperature was determined by a Si diode and controlled by a closed-cycle He refrigerator, a resistive heater, and a feedback system.

### III. RESULTS AND DISCUSSION

Figure 1(a) shows a set of IXS energy scans at  $(1/2, 1/2, 3/2)$ , which corresponds to an  $R$  point in the Brillouin zone. At  $T = T_C + 49$  K (far above the transition temperature), the spectrum shows two phonon peaks that correspond to phonon emission (positive energy) and phonon absorption (negative energy) with an intensity ratio determined by the usual Stokes–anti-Stokes ratio. As the temperature lowers, the two

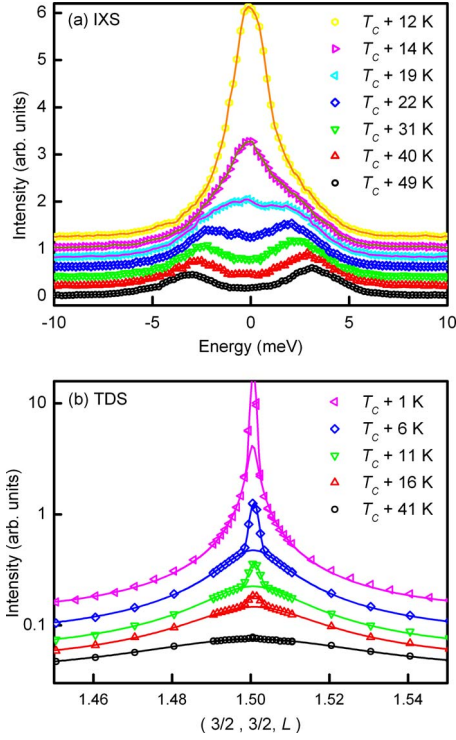


FIG. 1. (Color online) (a) IXS energy scans at  $(1/2, 1/2, 3/2)$  taken at various temperatures. Positive energy corresponds to phonon emission. The data points are connected by curves. (b) TDS scans in reciprocal space along an  $M$ - $R$ - $M$  line taken at various temperatures. The curves show the decomposition into a broad component and a narrow component.

phonon peaks move closer. The decreasing phonon energy signifies a softening of the mode; this is the lowest transverse-acoustic mode at the  $R$  point. Simultaneously, the CP emerges and gains intensity rapidly as  $T$  approaches  $T_C$ . For comparison, Fig. 1(b) shows TDS scans along an  $M$ - $R$ - $M$  line in reciprocal space centered about the  $R$  point at  $(3/2, 3/2, 3/2)$ .<sup>12</sup> At  $T=T_C+41$  K (far above the transition temperature), the spectrum shows a broad thermal peak that can be related to the soft mode and a barely noticeable NC right at the  $R$  point. As the sample temperature lowers, the broad thermal peak becomes more intense because of the decreasing soft-mode frequency and correspondingly increasing phonon populations around the  $R$  point. The NC also becomes more intense; it eventually evolves into a Bragg peak for  $T$  below  $T_C$ .

Figure 2 shows the energy of the soft phonon mode as a function of temperature determined from IXS measurements at the  $R$  point. It was not feasible to extract the phonon energy at temperatures very close to  $T_C$  directly from such IXS scans where the phonon peaks overlap substantially with the intense CP. The two data points at 108 and 113 K were, in fact, determined by extrapolation from scans with various detuning in reciprocal space away from the  $R$  point. The detuning increases the phonon energy, but more importantly it reduces the CP intensity, making it possible to determine the phonon energies. The results shown in Fig. 2 are in good agreement with earlier NS and TDS results.<sup>6,12</sup> The dashed curve is a mean-field fit based on

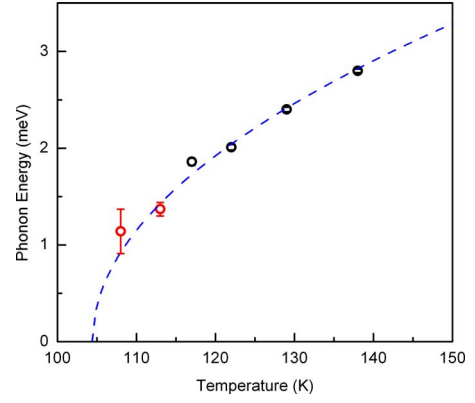


FIG. 2. (Color online) Energy of the soft mode as a function of temperature determined from IXS measurements at the  $R$  point except for the two data points at 108 and 113 K. These two points were determined by extrapolation from scans with various detuning in reciprocal space away from the  $R$  point. The dashed curve is a fit based on a mean-field model.

$$\hbar\omega = A\sqrt{T - T_C}, \quad (1)$$

where  $A=0.487 \text{ meV K}^{-1/2}$ .<sup>6</sup> It is known that renormalization effects are strong in this system, and a mean-field fit does not describe the soft-mode behavior accurately at temperatures very close to  $T_C$ .<sup>7,12</sup> The data point at 108 K is near the borderline where renormalization effects become significant.

Figure 3 shows IXS energy scans at  $T=108$  K for various detuning in reciprocal space from the  $R$  point at  $(1/2, 1/2, 3/2)$  with the detuning defined as  $\Delta\mathbf{q} = (-\Delta H, \Delta H, 0)$ . Data such as these constitute essentially a measure of the scattering function  $S(\mathbf{q}, \omega)$ . As  $\Delta H$  increases, the CP loses its intensity very rapidly and the phonon peaks move apart. Fitting all

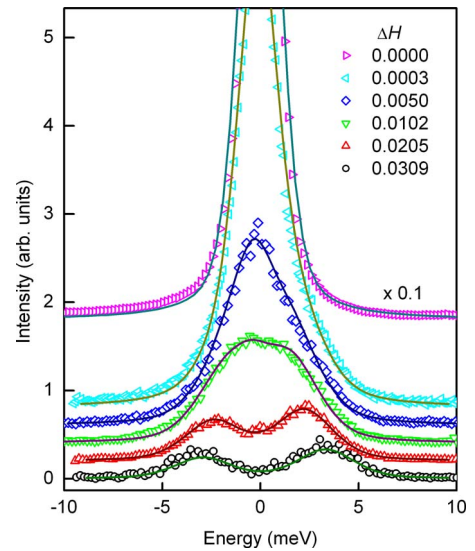


FIG. 3. (Color online) IXS energy scans at  $T=108$  K for various detuning  $\Delta H$  in reciprocal space from the  $R$  point at  $(1/2, 1/2, 3/2)$ . The symbols are data points, while the curves are fitting results.

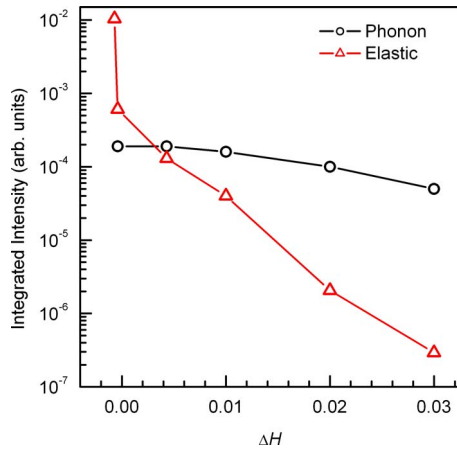


FIG. 4. (Color online) Integrated intensities from the phonon and elastic contributions to IXS scans at 108 K for various detuning  $\Delta H$  from the  $R$  point. The intensity scale is logarithmic.

spectra simultaneously with appropriate line shapes and constraints for the various components, we can separate the phonon contribution from the CP contribution. The fitting can become uncertain when the peaks overlap. In order to extract the information reliably, we have imposed a constraint on the phonon frequency based on an expansion of the phonon-dispersion curve for a soft mode<sup>6</sup>

$$\omega(\Delta q)^2 = \omega(\Delta q = 0)^2 + \alpha \Delta q^2, \quad (2)$$

where  $\alpha$  and  $\omega(0)$  are treated as fitting parameters. From the fitting, it is found that the phonon peak width is somewhat larger than the resolution function, while the CP has a resolution-limited peak width.

The results of this fitting analysis are presented in Fig. 4, which is essentially a TDS scan resolved into an elastic component and an inelastic (phonon) component. Note that the vertical intensity scale is logarithmic. The phonon component shows a smooth behavior as expected. Its intensity increases for decreasing detuning; this is because of an increasing phonon population for a decreasing phonon frequency according to Eq. (2). The elastic component, or the contribution from the CP, is strongly peaked at the  $R$  point ( $\Delta H=0$ ), with a width determined by the resolution function of the measurement. It has a tail extending into larger  $\Delta H$ , but the intensity is generally negligible compared to the phonon contribution. For instance, the elastic contribution is just about 1% of that from the phonon contribution at  $\Delta H=0.02$ , and it is about four orders of magnitude below the value at  $\Delta H=0$ . In contrast, NS shows a much broader width of the CP in reciprocal space; a significant intensity of the CP can still be seen at this detuning.<sup>6</sup>

The above x-ray results demonstrate that the NC is the same as the elastic component except for some minor tailing of the latter. Since the elastic component is entirely derived from the CP, we have established that the NC and CP are different manifestations of the same scattering mechanism. What is this scattering mechanism? Since standard phase transition theories for pure systems do not yield either a NC or a CP, even with renormalization and fluctuation effects

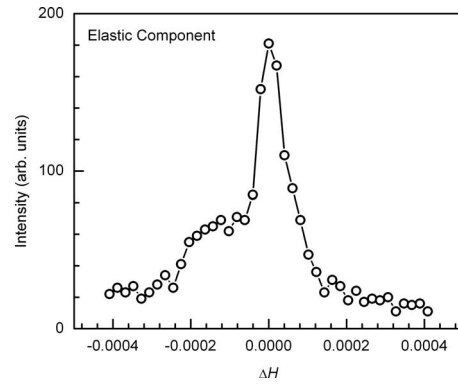


FIG. 5. Rocking curve of the elastic component ( $\Delta E=0$ ) around the  $R$  point with the sample temperature at 108 K. Note the much smaller range of momentum detuning compared to Fig. 4. The intensity scale is linear.

taken into account, the only reasonable explanation available is that these are caused by imperfections in the system. As transmission electron microscopy results have shown, commonly available  $\text{SrTiO}_3$  crystals contain defects.<sup>10</sup> The imperfect structure is also revealed by static and position-dependent x-ray speckle patterns at  $T$  above  $T_C$ .<sup>12,13</sup> Such defects can conceivably cause changes in  $T_C$  locally, resulting in the formation of regions with frozen phonons already at  $T > T_C$ . These regions give rise to a NC that is essentially a superlattice Bragg peak from the affected domains. The same scattering mechanism gives rise to the CP in IXS energy scans.

As further evidence, Fig. 5 presents a high-resolution rocking curve of the elastic component at 108 K taken around the same  $R$  point; the energy transfer  $\Delta E$  is set to zero within the IXS detector energy resolution. Note that the range of  $\Delta H$  for this scan is much smaller than the corresponding range shown in Fig. 4. The results show that the CP is extremely sharp as a function of detuning in reciprocal space. However, its detailed line shape is complicated. While it appears to consist of two main peaks separated by about  $0.008^\circ$ , the smaller peak is wider than the other, and there are extra scattering intensities that cannot be described by just two peaks alone. This complicated structure can be attributed to a mosaic spread and is consistent with the interpretation that the CP is caused by imperfections in the system rather than an intrinsic dynamic effect. This mosaic spread is also evident in results from complementary speckle measurements.<sup>12,13</sup>

The case for x-ray scattering from  $\text{SrTiO}_3$  is thus clear. The question is then: Why did NS fail to detect the NC? There are two possible reasons. One is that NS probes the whole volume of the sample ( $\sim 1 \text{ cm}^3$ ), as opposed to x-ray scattering, which probes a thickness on the order of 0.1 mm. It is possible that the defect structures responsible for the CP and NC in x-ray scattering are distributed only near the sample surface.<sup>6,9,10</sup> This is conceivable if the defects are caused by preparation of the sample surface including mechanical polishing. Assuming this, NS might be probing different kinds of defects that are more characteristic of the bulk material. But then, what kind of defect structure would give rise to a CP but no NC? Since the CP intensity rises rapidly

with  $T$  approaching  $T_C$ , the scattering mechanism must involve either an increasing scattering volume or an increasing number of scattering centers. The lack of a NC from NS would imply an increase in the number of uncorrelated scattering centers with such small dimensions for each to yield a scattering line width in reciprocal space indistinguishable from the broad phonon component.

A second explanation is that the momentum resolution of NS is typically much less than that of x-ray scattering. It is possible that the very sharp NC, as seen in Fig. 1(b), is smeared out and becomes difficult to separate from the broad phonon component. Either one or both mechanisms discussed above might account for prior NS results from SrTiO<sub>3</sub>.

#### IV. CONCLUSIONS

In summary, we have performed IXS measurements from SrTiO<sub>3</sub> to clarify the connection between the CP and NC near the  $R$  point for the displacive phase transition at  $T_C \sim 105$  K. Essentially all solid-state materials, including commercial wafers widely employed as electronic substrates, contain defect structures that can affect the material proper-

ties. X-ray scattering has such a high sensitivity that even minute amounts of defects can be readily detected near a phase transition, where the effects of defect structures are amplified. Using IXS, we have decomposed the TDS line shape from SrTiO<sub>3</sub> into elastic and phonon contributions. The elastic component has a very narrow width in reciprocal space, but its line shape is complicated. Our results show conclusively that both the CP and NC are present, and they are derived from the same scattering mechanism, namely, scattering by defect structures. This finding ends a long debate.

#### ACKNOWLEDGMENTS

This research was supported by the U.S. Department of Energy, Office of Science, Office of Basic Energy Science, under Contract No. DE-AC02-06CH11357 (H.H.) and Grant No. DE-FG02-07ER46383 (T.-C.C.). We acknowledge partial support of personnel and equipment in connection with the beamline operations by the National Science Foundation (Grant No. DMR-05-03323) and the Petroleum Foundation Fund administered by the American Chemical Society.

<sup>1</sup>H. Unoki and T. Sakudo, J. Phys. Soc. Jpn. **23**, 546 (1967).

<sup>2</sup>P. A. Fleury, J. F. Scott, and J. M. Worlock, Phys. Rev. Lett. **21**, 16 (1968).

<sup>3</sup>R. A. Cowley, W. J. L. Buyers, and G. Dolling, Solid State Commun. **7**, 181 (1969).

<sup>4</sup>T. Riste, E. J. Samuelsen, K. Otnes, and J. Feder, Solid State Commun. **9**, 1455 (1971).

<sup>5</sup>S. M. Shapiro, J. D. Axe, G. Shirane, and T. Riste, Phys. Rev. B **6**, 4332 (1972).

<sup>6</sup>G. Shirane, R. A. Cowley, M. Matsuda, and S. M. Shapiro, Phys. Rev. B **48**, 15595 (1993).

<sup>7</sup>S. R. Andrews, J. Phys. C **19**, 3721 (1986).

<sup>8</sup>D. F. McMorrow, N. Hamaya, S. Shimomura, Y. Fujii, S. Kishimoto, and H. Iwasaki, Solid State Commun. **76**, 443 (1990).

<sup>9</sup>K. Hirota, J. P. Hill, S. M. Shapiro, G. Shirane, and Y. Fujii,

Phys. Rev. B **52**, 13195 (1995).

<sup>10</sup>R. Wang, Y. Zhu, and S. M. Shapiro, Phys. Rev. Lett. **80**, 2370 (1998).

<sup>11</sup>H. Hünnefeld, T. Niemöller, J. R. Schneider, U. Rütt, S. Rodewald, J. Fleig, and G. Shirane, Phys. Rev. B **66**, 014113 (2002).

<sup>12</sup>M. Holt, M. Sutton, P. Zschack, H. Hong, and T.-C. Chiang, Phys. Rev. Lett. **98**, 065501 (2007).

<sup>13</sup>S. Ravy, D. Le Bolloc'h, R. Currat, A. Fluorasu, C. Mocuta, and B. Dkhil, Phys. Rev. Lett. **98**, 105501 (2007).

<sup>14</sup>H. Sinn, E. E. Alp, A. Alatas, J. Barraza, G. Bortel, E. Burkel, D. Shu, W. Sturhahn, J. P. Sutter, T. S. Toellner, and J. Zhao, Nucl. Instrum. Methods Phys. Res. A **467-468**, 1545 (2001).

<sup>15</sup>T. S. Toellner, A. Alatas, A. Siad, D. Shu, W. Sturhahn, and J. Zhao, J. Synchrotron Radiat. **13**, 211 (2006).